Thermal Total Cross Sections of Europium from Neutron Capture and Transmission Measurements

G.Leinweber, D.P. Barry, R.C. Block, M.J. Rapp, and J.G. Hoole
Bechtel Corp., Knolls Atomic Power Laboratory, P.O. Box 1072, Schenectady, New York 12301 email: leinwg@rpi.edu

Y. Danon, R.M. Bahran, and D.G. Williams
Gaerttner LINAC Center, Rensselaer Polytechnic Institute, Troy, New York 12180

J.A. Geuther
Kansas State University, 3002 Rathbone Hall, Manhattan, Kansas 66506

F.J. Saglime III
Moog Inc., East Aurora, New York 14052

INTRODUCTION

Europium is a fission product in the low-yield tail at the high end of the fission fragment mass distribution. The stable isotopes have mass numbers 151 and 153. Of the rare earth metals, europium is the most reactive in air, making it a challenge to prepare samples in metallic form. ^{151}Eu and ^{153}Eu are lanthanides with substantial thermal neutron absorption cross section. It is therefore of interest for its role as a neutron absorber in nuclear reactors. Transmission measurements are not sensitive to the efficiency of the detector or a precise knowledge of the neutron flux. At 0.0253 eV neutron interactions with europium are >96% neutron capture. Therefore, neutron capture measurements were augmented with transmission measurements of thermal total cross section.

DETERMINING THERMAL CROSS SECTION AND UNCERTAINTY

Total cross sections were determined from transmission and capture measurements at the Rensselaer Polytechnic Institute (RPI) linear electron accelerator (LINAC) using natural and ^{153}Eu-enriched encapsulated metal samples.

Sample images were obtained via x-ray analysis and used to get the area of each sample. Each sample was weighed to determine its mass before encapsulation. Transmission sample details are shown in Table I including sample thickness, isotopic content, measured thermal (0.0253 eV) total cross section, and the energy interval over which it was determined for transmission. Table II gives the same information for the samples used in the capture measurement. The thickest ^{153}Eu-enriched sample (sample number 1) was a stack of the two thinner ^{153}Eu-enriched samples (sample numbers 2 and 5).

The ^{153}Eu-enriched samples were prepared at Oak Ridge National Laboratory and were measured shortly after production. X-ray images of the samples were made at various times in the months following production;

Table I. Transmission Sample Details and Cross Sections

Sample number	1	2	3	4
Nominal thickness (mils)	15	5	10	5
Sample thickness (at/b x 10^{-4})	7.16 ± 0.20	2.42 ± 0.11	4.52 ± 0.15	2.55 ± 0.27
Atom fraction (f_i^{151})	0.0123± 0.0002	0.0123± 0.0002	0.4781± 0.0003	0.4781± 0.0003
Atom fraction (f_i^{153})	0.9877± 0.0002	0.9877± 0.0002	0.5219± 0.0003	0.5219± 0.0003
σ_i, barns	491 ± 3	510 ± 6	4978 ± 30	4519 ± 30
ΔE, eV	.00136	.00214	.00020	.00020

Table II. Capture Sample Details and Cross Sections

Sample number	1	2	5 (see Fig. 1)	4
Nominal thickness (mils)	15	5	10	5
Sample thickness (at/b x 10^{-4})	7.16 ± 0.20	2.42 ± 0.11	4.74 ± 0.17	2.55 ± 0.27
Atom fraction (f_i^{151})	0.0123± 0.0002	0.0123± 0.0002	0.0123± 0.0002	0.4781± 0.0003
Atom fraction (f_i^{153})	0.9877± 0.0002	0.9877± 0.0002	0.9877± 0.0002	0.5219± 0.0003
σ_i, barns	463 ± 2	439 ± 2	480 ± 3	5049 ± 19
ΔE, eV	.00103	.00195	.00057	.00103

sample degradation and non-uniformities were noted and are documented in Reference (1). An x-ray image of the nominal 10-mil-thick (1 mil = 0.001 in) ^{153}Eu-enriched sample measured in both transmission and capture is shown in Fig. 1. The pinhole visible in the sample affects the measured cross section by <1%.

The thermal total cross sections were derived directly from the measured data. No formalism or resonance parameter extraction computer program was required. The cross section uncertainty was estimated by propagating the counting statistics from transmission and capture measurements. Furthermore, differences between samples have been incorporated into the analysis through a weighted least squares fit. An external uncertainty[2] was established to quantify the difference between transmission and capture results.

The Experimental Parameters

The Rensselaer Polytechnic Institute (RPI) LINAC is a 60-MeV electron accelerator producing ~10^{13} neutrons isotropically from a Ta target. Thermal transmission was measured at a flight path length of ≈15 m using a ^{6}Li glass scintillation detector.[3,4] The dead time for the system was 0.28 μs.

Thermal neutron capture was measured at a flight path length of ≈25 m using a multisegment NaI detector.[3,4,5] The dead time for the system was 1.125 μs.

Transmission and capture experiments utilized the same neutron-producing target and time-of-flight clock. The target was specially-designed to enhance the thermal energy region.[6,7] The clock was a FAST Comtec P7889 multichannel scaler. The repetition rate of the accelerator was 25 pulses per second, giving time to measure incident neutron energies down to 10 meV. Beam monitors were used to correct for beam intensity fluctuations.

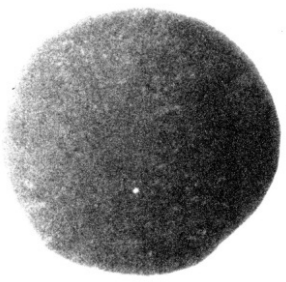

Fig. 1.X-ray image of the sample #5 (see Table II), the 10-mil-thick ^{153}Eu-enriched sample. Nonuniformities are visible in the sample that contribute to uncertainties in the measured cross sections. The apparent pinhole near the center of the sample affects transmission <1%.

Measuring Background

The background counting rate in transmission was known at ≈18 eV from a 10-mil-thickfixed tungsten notch, placed in the neutron beam throughout the measurement. The shape of the background in time-of-flight was measured using the black filter method where single- and double-thicknesses of selected notch filters were inserted into the beam for some of the run time. The saturated background notch counting rates were extrapolated to zero thickness to establish the shape of the neutron background.[8]Absolute background counting rates were established by normalizing the background shape at the fixed notch.

The neutron capture background was measured with an empty Al sample holder.

Measuring Neutron Flux in the Capture Measurement

The neutron flux was measured using a 100-mil-thick boron carbide sample enriched to 98.4% in ^{10}B. It absorbs >99.9% of the flux at 0.0253 eV. The flux shape was normalized to the saturated capture resonance at 0.46 eV in ^{151}Eu.

Cross Section Analysis Method

Thermal total cross sections for ^{151}Eu and ^{153}Eu, σ^{151} and σ^{153}, were determined from transmission and capture measurements independently. Then the results were combined along with their uncertainties using the following procedure.

1) Determine cross section for all samples, elemental and enriched.
2) Perform a weighted least squares fit of cross section vs sample enrichment. The result was σ^{151} and $\sigma^{153}$for transmission and a second result for capture
3) Transmission and capture total thermal cross section results were combined into a variance-weighted average and uncertainty.

Eqns (1) and (2) relate transmission, *T*, to total cross section.

$$T = exp\,(-N\sigma_{tot}) \quad (1)$$

so,

$$\sigma_{tot} = \frac{-ln\,(T)}{N} \quad (2)$$

Where *N* is sample thickness in atoms/barn. The σ_{tot} can be calculated directly, and the results are shown in Table I at 0.0253 eV averaged over ΔE.

Capture data were reduced to capture yield, *Y*. The capture yield is related to total cross section, σ_{tot}, capture

cross section, σ_γ, and scattering cross section, σ_s, according to Eqns (3), (4), and (5).

$$Y = (1 - exp(-N\sigma_{tot}))\frac{\sigma_\gamma}{\sigma_{tot}} \quad (3)$$

$$\sigma_{tot} = \frac{-ln\,[1-(\frac{\sigma_{tot}}{\sigma_\gamma})Y]}{N} \quad (4)$$

and

$$\sigma_{tot} = \frac{-ln\,[1-(\frac{\sigma_{tot}}{\sigma_{tot}-\sigma_s})Y]}{N} \quad (5)$$

The thermal total cross section, σ_{tot}, in Eqn (5) was solved for numerically using the measured capture yield, Y, and the published values for the scattering cross sections[9] (σ_s=6.3 barns for ^{151}Eu and σ_s=10.7 barns for ^{153}Eu). The initial estimate for σ_{tot} was taken from ENDF/B-VII.1.[10] The final σ_{tot} results and their uncertainties for each sample are given in Tables I and II.

Cross Sections from Each Sample

The total cross sections for each sample at each measured energy point were determined using Eqns (2) and (5). The uncertainty in each cross section was propagated from counting statistics. A procedure was developed to determine the optimal number of data points, ΔE in Tables I and II, to include for each sample's average thermal total cross section, σ_i. At successively wider energy intervals the standard deviation of the distribution of σ_i values was compared to the uncertainty from the counting statistics at 0.0253 eV. The uncertainty in total cross section, $\Delta\sigma_i$, was not reduced as the energy interval was widened. An energy interval was chosen such that the standard deviation of the mean of the distribution of σ_i values equaled the uncertainty on the central point determined from counting statistics. That uncertainty was cited as the uncertainty in the total thermal cross section for sample i, $\Delta\sigma_i$. Equating the two sources of uncertainty (counting statistics at 0.0253 eV and the width of the distribution of σ_is in the interval ΔE) produced the best central value of σ_i. Table I gives the cross section for each sample in transmission, its uncertainty, and the energy interval, ΔE, centered at 0.0253 eV, used to determine σ_i. Table II gives the same information from the capture measurement.

Conceptually, σ_γ can be derived from Eqn (4) using capture data, knowing σ_{tot} from the transmission results. Furthermore, the scattering cross section could be determined from the difference between the capture cross section and the total cross section. However, the difference between the total cross section from transmission data (Table I) and the capture data (Table II) for sample numbers 1, 2, and 4, common to both experiments, is considered to be due more to systematic uncertainties in the measurements rather than an accurate measure of the scattering cross section.

Fit ^{151}Eu and ^{153}Eu Thermal Total Cross Section

The cross section for each sample, σ_i, is described by Eqn (6).

$$\sigma_i = f_i^{151}\ \sigma^{151}\ + f_i^{153}\ \sigma^{153}\ \text{, i=1..4} \quad (6)$$

where f_i^{151} and f_i^{153} are given in Tables I and II. σ^{151} and σ^{153} are the desired quantities, thermal total cross sections of ^{151}Eu and ^{153}Eu, respectively. The system of four equations for transmission was solved for the two unknowns, σ^{151} and σ^{153}. The same was done for capture. Eqn (6) can be rearranged into the following system of linear Equations.

$$y_i = ax_i + b \quad (7)$$

where

$$x_i = \frac{f_i^{153}}{f_i^{151}},\quad y_i = \frac{\sigma_i}{f_i^{151}},$$

$a=\sigma^{153}$, and $b=\sigma^{151}$.

The points were plotted on the xy plane (see Fig. 2). A least squares fit was made to transmission and capture data separately, including the propagation of the uncertainties given in Tables I and II. The results are given in Table III. The weighted fit implicitly accounts for any disagreement between samples.

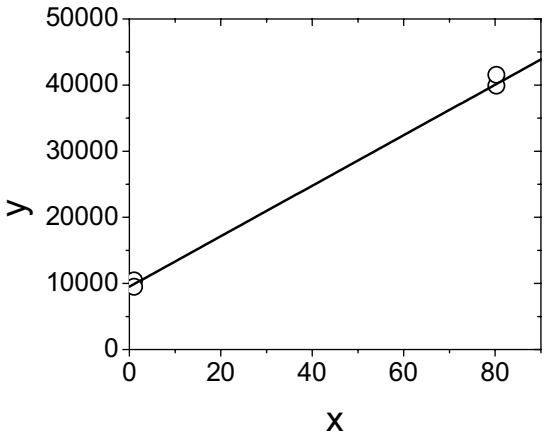

Fig. 2. Plot of fitting parameters defined by Eqn (7). The y axis is proportional the sample cross section (σ_i), and the x axis is the ratio of isotopic atom fractions. A weighted linear fit to each revealed the slope=σ^{153}, and the y intercept=σ^{151} (see Table III). An analogous plot was made from capture data.

Table III. Eu Cross Section Results

	^{151}Eu Thermal Total Cross Section, σ^{151} (barns)	^{153}Eu Thermal Total Cross Section, σ^{153} (barns)
Transmission	9500 ± 50	382 ± 3
Capture	10200 ± 40	336 ± 2
Final combined transmission and capture	9900 ± 350	340 ± 20
ENDF/B-VII.0[9] Error from Mughabghab[10]	9200 ± 100	321 ± 8
ENDF/B-VII.1[11] Error from Mughabghab[10]	9200 ± 100	367

Combining the Transmission and Capture Results

The thermal total cross sections for each type of experiment, σ_j, and their uncertainties, $\Delta\sigma_j$, are given in Table III. The average thermal total cross section, $\bar{\sigma}$, was derived from the values in Table III using Eqn (8).

$$\bar{\sigma} = \frac{\sum_{j=1}^{2} \frac{\sigma_j}{(\Delta\sigma_j)^2}}{\sum_{j=1}^{2} \frac{1}{(\Delta\sigma_j)^2}} \qquad (8)$$

where j is the index on experiment type, transmission or capture. The uncertainty in the average thermal total cross section, $\Delta\bar{\sigma}$, was calculated from two sources, the propagated counting statistics and the external uncertainty[2], defined in Eqn (9).

$$\Delta\sigma_{external} = \sqrt{\frac{\sum_{j=1}^{2} \frac{(\bar{\sigma} - \sigma_j)^2}{(\Delta\sigma_j)^2}}{\sum_{j=1}^{2} \frac{1}{(\Delta\sigma_j)^2}}} \qquad (9)$$

The final combined transmission and capture results are given in Table III. The one-sigma uncertainty on the final combined transmission and capture cross section is the larger of the two sources of uncertainty. In this case the final combined uncertainty is dominated by the external uncertainty. The average cross section, $\bar{\sigma}$ in Eqn. (8), is weighted by the counting statistics of the measurements. The central value depends on the particular samples and the measurement time spent on each. The external uncertainty, $\Delta\sigma_{external}$ in Eqn. (9), does not change substantially when the counting time of any measurement is increased because it is dominated by the differences between the individual measurements, $(\bar{\sigma} - \sigma_j)^2$. The final combined transmission and capture cross sections in Table III are bounded by the quoted uncertainties.

DISCUSSION

Table III shows a comparison of the most recent ENDF evaluations to the current results The increase in total thermal cross section for ^{153}Eu from ENDF/B-VII.0[9] to ENDF/B-VII.1[11] was partially due to the work of Dean et al. and Mughabghab.[12] The current results for ^{153}Eu are within the 1σ uncertainty band of ENDF/B-VII.0[9] in the direction of the ENDF/B-VII.1[11] revision.

The thermal total cross sections of europium were determined from neutron capture and transmission measurements using samples enriched in ^{153}Eu, as well as, elemental samples. The samples were difficult to form and are highly reactive (see Fig. 1). Variations in thickness in particular regions of the samples were not taken into account. No uncertainty in sample thickness was explicitly included in the analysis. Rather, differences in results between samples and between transmission and capture measurements have been propagated into the final results, given in Table III. The uncertainties on the thermal total cross sections were 3.5% for ^{151}Eu, and 6% for ^{153}Eu.

ENDNOTES

The authors would like to thank accelerator engineer Peter J. Brand and his staff Matthew C. Gray, Martin R. Strock, and Azeddine Kerdoun for the exemplary performance of their duties at the Gaerttner LINAC Center at RPI. Without their unique skills this work would not have been possible.

REFERENCES

1. R.C. BLOCK, J.A. GEUTHER, B. METHE, D.P. BARRY, G. LEINWEBER, "X-ray Determination of the Thickness of Thin Metal Foils," submitted to *NIM A*, (2012).
2. Y. DANON et al., "Beryllium and Graphite High Accuracy Total Cross-Section Measurements in the Energy Range from 24 keV to 900 keV," *Nuc. Sci &Eng.*, **161**, 321 (2009).
3. R.E. SLOVACEK et al., "Neutron Cross-Section Measurements at the Rensselaer LINAC," *Proc. Topl. Mtg. Advances in Reactor Physics*, Knoxville, Tennessee, April 11-15, (1994)
4. R.C. BLOCK, et al., "Neutron Time-of-Flight Measurements at the Rensselaer LINAC," *Proc. Int. Conf. Nuclear Data for Science and Technology*, Gatlinburg,

Tennessee, May 9-13, 1994,**1**, 81, American Nuclear Society (1994).
5. R.C. BLOCK, et al., "A Multiplicity Detector for Accurate Low-Energy Neutron Capture Measurements," *Proc. Int. Conf. Nuclear Data for Science and Technology*, Mito, Japan, p. 383 May 30-June 3, (1988).
6. Y. DANON, R.E. SLOVACEK, and R.C. BLOCK, "The Enhanced Thermal Neutron Target at the RPI LINAC," Trans. Am. Nucl. Soc., **68**, 473 (1993).
7. Y. DANON, R.E. SLOVACEK, and R.C. BLOCK, "Design and Construction of a Thermal Neutron Target for the RPI LINAC," Nucl. Instrum. & Methods Physics Research A, **352**, 596 (1995).
8. D.B. SYME, "The Black and White-Filter Method for Background Determination in Neutron Time-of-Flight Spectrometry," Nucl. Instrum.& Methods, **198**, 357 (1982).
9. M.B. CHADWICK et al., "ENDF/B-VII.0: Next Generation Evaluated Nuclear Data Library for Science and Technology," *Nuclear Data Sheets*, **107**, 12, 2931 (2006).
10. S.F. MUGHABGHAB, Atlas of Neutron Resonances, 5th ed., Elsevier, New York (2006).
11. M.B. CHADWICK et al., "ENDF/B-VII.1: Nuclear Data for Science and Technology: Cross Sections, Covariances, Fission Product Yields and Decay Data," *Nuclear Data Sheets*, **112**, 2887 (2011).
12. S.F. MUGHABGHAB, "Analysis of Measurements in the Unresolved Resonance Region for ENDF Evaluations," *RPI Nuclear Data (RND) 2011 Symposium for Criticality Safety and Reactor Applications,* Troy, New York, April 27, (2011).